39th IAHR WORLD CONGRESS GRANADA, SPAIN 2022 From Snow to Sea 19-24 June 2022

Proceedings of the 39th IAHR World Congress
19–24 June 2022, Granada, Spain
doi://10.3850/IAHR-39WC2521716X20221816

Numerical Approach for the Evaluation of Downstream Fish Guiding at Low-Head Hydropower Plants

Hannes Zöschg[(1)], Bernhard Zeiringer[(2)], Günther Unfer[(3)], Ruben Tutzer[(4)] and Markus Aufleger[(5)]

[(1,4,5)] Unit of Hydraulic Engineering, University of Innsbruck, Innsbruck, Austria,
hannes.zoeschg@uibk.ac.at; ruben.tutzer@uibk.ac.at; markus.aufleger@uibk.ac.at

[(2,3)] Institute of Hydrobiology and Aquatic Ecosystem Management, University of Natural Resources and Life Sciences, Vienna, Austria,
bernhard.zeiringer@boku.ac.at; guenther.unfer@boku.ac.at

Abstract

When migrating downstream, fish usually follow the main current, which typically leads them to the turbines of hydropower plants (HPPs). When fish pass through the turbines, they can be injured or even killed. To prevent fish damage, fish guidance structures (FGS) in combination with bypass-systems provide a safe downstream migration corridor. However, the fish guiding efficiency (FGE) as well as the fish protection efficiency (FPE) of such structures are largely dependent on species- and site-specific conditions. In the design of new HPPs as well as in the ecological adaption of existing ones, there is no general solution for the implementation of FGS. Instead, the “trial and error” approach is often used. To investigate the influence of specific geometric and hydraulic parameters of HPPs on downstream migrating fish, a 3D numerical approach using the software ANSYS Fluent 19 was applied in this study. The flow conditions upstream of simplified HPPs were simulated and evaluated regarding FGE and FPE. Based on a parameter analysis, general results were derived, e.g. concerning the effects of rake angle or design type of HPPs. Furthermore, the present study illustrates the importance of investigating the flow conditions and evaluating FGE and FPE in the planning of appropriate measures at HPPs.

Keywords: Sustainable hydropower; Fish protection; Fish downstream migration; 3D numerical simulations; Computational fluid dynamics

1. INTRODUCTION

Hydropower is an essential component of electricity production in many countries around the world, especially in countries with large water resources and significant topographic differences in altitude. In Austria, for example, the share of hydropower in gross electricity generation ranged from 55% to 67% between 2005 and 2019, depending on variable generation conditions (BMK, 2020). However, there is also increasing criticism of hydropower because of its negative consequences for river ecology. This concerns the interruption of the longitudinal continuity of free-flowing rivers in particular. Besides restricting the natural sediment transport, the migratory behavior of fish and other aquatic organisms is disturbed, and habitats get disconnected. In the long term, this can lead to a decrease in fish populations or even the extinction of species from certain rivers of river reaches (BMLFUW, 2017). The EU Water Framework Directive demands the maintenance or restoration of river continuity in Europe (European Commission, 2000). While appropriate technical measures have already been implemented to enable upstream fish migration at several hydropower plants (HPPs) in Europe, the problem of downstream migration remained unrecognized for a long time (BMLFUW, 2012).

In the planning of new HPPs as well as in the ecological adaptation of existing HPPs, it is important to ensure that fish can safely migrate downstream. Since fish are known to follow the main current leading to the turbines during normal operation of HPPs, they can be injured or even killed when passing the turbines (Ebel, 2018). In this context, fish guiding structures (FGS) in combination with a bypass system are a suitable way to avoid turbine passage. As an FGS, a trash rack with horizontal bar racks (HBR) or vertical bar racks (VBR) can be used as a physical barrier with small clear bar spacing and is therefore physically impermeable to most fish. If the trash rack is installed with a horizontal angle α to the incoming flow, fish can be guided to the bypass inlet. The bypass should be located at the lower end of the FGS so that it can be easily found by the fish. In addition, flow conditions should be as uniform as possible without exceeding critical limits into the bypass to provide an attracting flow for fish (Ebel, 2018).

To investigate the complex hydraulic conditions as well as to optimize fish protection at run-of-river HPPs, 3D numerical simulations have already been used in previous studies. For example, Feigenwinter et al. (2019) simulated flow conditions at a HPP in Switzerland and determined potentially optimized positions of

FGS based on the evaluation of cross sections. Furthermore, Szabo-Meszaros et al. (2019) combined simulated hydraulic conditions at a HPP in Norway with measured fish migration data to examine various measures for the optimization of downstream fish migration past the hydropower intake.

However, due to species- and site-specific conditions, there are no general solutions for the positioning of FGS in combination with a bypass at run-of-river HPPs. More often, the "trial and error" approach is used (Katopodis and Williams, 2012), which is sometimes followed by further revisions and therefore can lead to high financial costs and increased time expenditure (Szabo-Meszaros et al., 2019). To address this issue, the present study investigates the flow conditions upstream of simplified run-of-river HPPs at potential sites in the Austrian Danube catchment using 3D numerical simulations. The study was conducted as part of a research project in which geometric and hydraulic parameters were varied based on a parametric analysis. Subsequently, the hydraulic conditions as well as the fish guidance efficiency (FGE) and the fish protection efficiency (FPE) were evaluated.

2. METHODS

2.1 Definition of The Relevant HPPs

In a first step, three fictional HPPs with low head between 2 and 5 meters were defined, considering potential sites in Austria in the catchment area of the Danube river. Based on a potential site of the river flow power plant as described by Aufleger and Brinkmeier (2010), a bay-type HPP (HPP I) was defined for a lowland river reach with a design flow of 225 m³/s (including fish protection and fish guidance structures). The site of this type is usually located in the barbel region and has the most abundant fish species (Haunschmid et al., 2006). For a pre-alpine river with a discharge of 50 m³/s in the grayling region, a block-type HPP (HPP II) was defined. Further, another block-type HPP (HPP III) was defined for an alpine river reach with a discharge of 10 m³/s in the lower trout region. In the river sections of HPP II and HPP III, the number of fish species is significantly lower (Haunschmid et al., 2006). The HPP components powerhouse, dividing pier and weir were defined based on existing similar HPPs in Austria and combined with FGS and a bypass system. The angled bar rack bypass system designed by Ebel, Gluch & Kehl (2001) according to Ebel (2018) was used as a reference, which has already been implemented at several HPPs in Europe (Ebel, 2020). For the defined HPPs, basic assumptions were made in each case regarding the geometric and hydraulic parameters to obtain results as generally valid as possible. For example, the geometries were significantly simplified compared to real HPPs. In addition, constant discharges in the river and constant discharges through the turbines were assumed. Other HPP components such as a fish ladder or an alternative downstream corridor such as a residual flow over the weir were not considered in this study.

The main parameters of the defined HPPs are listed in Table 1, while the definition procedure as well as the created 3D models are shown in Figure 1.

Table 1. Main parameters of the relevant HPPs

HPP	LOCATION	CONSTRUCTION TYPE	DISCHARGE	WATER HEAD	NUMBER OF TURBINES
I	Lowland river	Bay-type HPP	225 m³/s	5 m	20
II	Pre-alpine	Block-type HPP	50 m³/s	4 m	6
III	Alpine	Block-type HPP	10 m³/s	2 m	3

For each of the three HPPs, several variations were defined with different geometrical and hydraulic parameters based on a parameter analysis. The focus of the study was particularly on the lower end of the FGS or the bypass inlet, respectively. In total, 52 variations were defined, numerically simulated and evaluated regarding the hydraulic conditions as well as the FGE and the FPE.

2.2 Numerical Modelling

The numerical simulations were performed with the software ANSYS Fluent 19. The hydraulic conditions in the computational domain were simulated by using a pressure-based solver (SIMPLE) that discretizes the Reynolds-averaged Navier-Stokes equations. The realizable k-ε turbulence model with scalable wall functions was applied to describe the turbulence kinetic energy and dissipation rate. The hydraulic conditions of HPP II and HPP III were simulated as a two-phase flow (water and air) using the volume of fluid (VOF) method, while a single-phase flow was considered for HPP I to minimize computational costs. An unstructured computational mesh was used to represent the complex geometries. The mesh sizes varied from 0.8 to 11 million elements depending on the HPP considered. The models were divided into several bodies to have a finer discretization of the computational mesh in areas of particular relevance, for example, in the vicinity of the FGS and at the bypass inlet. In order to ensure that the numerical results are independent from the cell sizes, a mesh

independency study was performed using the grid convergence index method (Celik et al., 2008). For this analysis, three different meshes have been tested with a refinement factor above 1.3 and for each mesh, the mean velocities at different positions in the domain were used as indicators. Finally, the cell size of 0.2 meters was used in the refined area, and 0.4 meters for the rest of the models. Close to the walls, inflation layers with a first layer thickness of 0.008 meters were used to accurately model the influence of the wall roughness on the flow field. For the chosen mesh, the Grid Convergence Index (GCI) was below 1% in all cases.

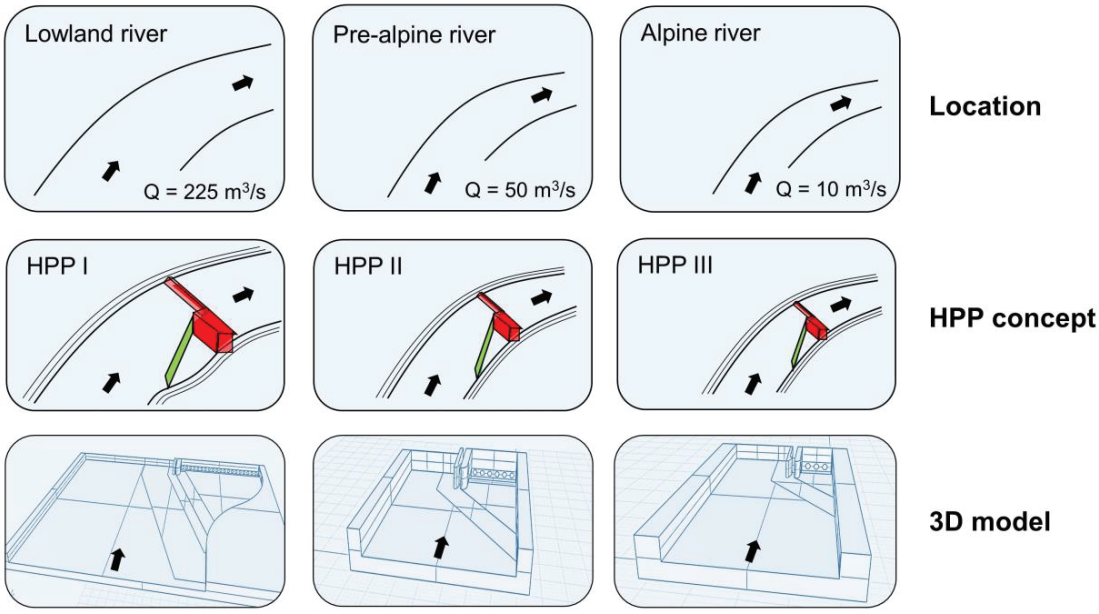

Figure 1. Schematic illustration of the approach used to define the locations and layouts of the HPPs (red: weir and powerhouse, green: FGS) with the 3D models created

Since the defined HPPs are fictional, a validation of the numerical models in the traditional way was not possible. For this reason, previous measurements at the HyTEC facility in Lunz am See, Austria, were used, where Haug (2018) performed velocity measurements in the context of ethohydraulic experiments. Based on these data, a 3D model of the facility was created, simulated and validated. The validated settings were subsequently transferred to the numerical models of the HPPs in this study.

To consider the hydrodynamic influence of FGS on the local flow field, a sufficiently refined mesh close to the bars is needed, leading to a very high computational effort (Feigenwinter et al., 2019). Consequently, FGS were not implemented in the computational domains of this study. Instead, a thin porous medium in the plane of the FGS was used in the numerical simulations, for which a used-defined function (UDF) was created. By implementing the UDF, a hydraulic loss coefficient is applied to each element in the porous medium as a function of the angle of inflow. This allows the consideration of the partially very different angles of inflow towards the trash rack or the porous medium, respectively. Empirical formulas from the literature were used to calculate the hydraulic loss coefficients as input data for the UDF, depending on the considered trash rack configuration.

2.3 Evaluation of Fish Protection and Fish Guidance

In order to evaluate the flow pattern resulting from the 3D numerical simulations, an assessment concept was applied with regard to aspects of fish behavior. This concept is mainly based on the velocity distributions and velocity vectors at different heights of the water head along the potential migration corridor close to the HPP. In particular, longitudinal defined areas along the FGS, the inlet area immediately upstream of the bypass and in the close range of the dividing pier, as well as the flow patterns within the bypass were evaluated separately. The key fish species occurring at the defined sites and relevant for the assessment were considered according to the defined fish biocoenosis for the river reaches (Haunschmid et al., 2006). Furthermore, the fish biocoenosis was divided into fish groups (guilds) with respect to downstream migration behavior, distinguishing especially between vertical migration height (migration at the bottom or at the water surface), fish size, swimming strength and life-stage (juveniles or adults).

Flow direction to the bypass inlet was defined as a main criterion in order to guide fish along a suitable downstream migration corridor. In general, a good FGE can be assumed if the tangential velocity (v_{tan}) is

greater than the normal velocity (v_{normal}) to the FGS ($v_{tan} > v_{normal}$). The angle of the incident flow α to FGS is thus smaller than 45° (Ebel, 2018). Another important criterion is the flow velocity along the FGS but also directly at the inlet area of the bypass. To avoid fish damage due to contact with the barrier, in areas with a low (i.e. α is greater than 45° and thus $v_{tan} < v_{normal}$) or no FGE ($v_{tan} = 0$, $\alpha = 90°$), the approach flow velocity has to be considered (Ebel, 2018). In addition to the FGE along the FGS, fish need to find the bypass. This should be achieved by a guiding flow directed towards the bypass inlet. Minimum requirements for velocities or velocity gradients immediately upstream of and in the bypass found in literature were considered (e.g. Ebel, 2018).

Based on these criteria, the velocity distributions and vectors were analyzed, the expected fish behavior was estimated, and thus the considered HPPs including different variations were evaluated with respect to FGE and FPE.

3. RESULTS & DISCUSSION

3.1 Overview

In the following, some results of the 3D numerical simulations are analyzed in terms of the velocity distribution (magnitude and direction). Furthermore, the FGE and the FPE are evaluated. Due to the large number of variations performed in the research project (Zöschg et al., 2021), only selected results are presented and discussed.

All variations presented below have some common characteristics: As a FGS, HBR are used. HBR obtain their guiding efficiency mainly through the rack angle and the physical barrier effect and have already been successfully implemented at several HPPs in Europe (Ebel, 2018). For the HBR, a bar thickness of 10 mm and a bar spacing of 10 mm were chosen. Thus, the blocking ratio of the HBR is 50%, which means that a relatively high effect on the flow conditions can be expected. Moreover, for the shape of the bars, a circular bar shape was used due to the relatively high hydraulic losses compared to hydrodynamically streamlined shapes (Meister, 2020). Another reason for using the circular bar shape was the already existing data based on previous physical model tests (Böttcher et al., 2019).

3.2 Effect of Rack Angle

Figure 2 shows the velocity vectors at the lower end of the FGS with an angle of (a) $\alpha = 40°$ and (b) $\alpha = 20°$ to the unaffected flow direction at the block-type HPP on the pre-alpine river (HPP II). Independent of the rack angle, the velocities are almost identical with respect to magnitude and direction. The flow conditions are hardly deflected by the rack angle. Therefore, this results in only a minor effect on the FGE. When considering the flow conditions along the entire FGS, it is noticeable that independently of the rack angle to the unaffected flow direction, low angles of inflow to the trash rack only occur at the upper end of the FGS. At the lower end, the vectors are almost perpendicular to the FGS due to the deflected flow towards the turbines, especially for the variation with $\alpha = 40°$. For $\alpha = 20°$, slightly lower angles occur and a marginally improved FGE arises. In addition, higher velocities at the lower end of the FGS appear for the variant with $\alpha = 40°$ compared to the variant with $\alpha = 20°$. This can be explained by the fact that at $\alpha = 20°$ the assumed tangential connection to the dividing pier shifts the FGS line to an area with lower flow velocities. Further, for both variants, the flow velocities at the lower end of the FGS are approximately twice as high as at the upper end.

Overall, the variant with $\alpha = 20°$ shows more favorable characteristics regarding the FGE over the entire length of the FGS compared to the variant with $\alpha = 40°$. However, in relation to other factors in the planning and operation of HPP with FGS and low rack angles, disadvantages can appear, for example, as a result of the higher costs in construction as well as the more difficult operation of rack cleaning machines due to the longer design.

3.3 Effect of Bottom Overlays

Figure 3 shows the velocity vectors in the vicinity of the FGS with $\alpha = 40°$ to the unaffected flow direction at the block-type HPP on the pre-alpine river (HPP II) (a) without a bottom overlay and (b) with a bottom overlay with a height of 0.2 m. The bottom overlay leads to a slightly greater deflection of the velocity vectors at the lower end of the FGS close to the bottom ($z = 0.1$ m; bottom at $z = 0.0$ m). Thus, the FGE is reduced. In the upper area of the FGS, the vector directions are deflected tangentially to the bottom overlay in direction of the bypass inlet. The flow velocities in front of the bottom overlay are only slightly reduced at near-bottom depth ($z = 0.1$ m). This may also be explained by the relatively low height of the defined bottom overlay compared to recommendations from the literature. For example, Ebel (2018) recommends a minimum height of 0.5 m for bottom overlays based on previous studies.

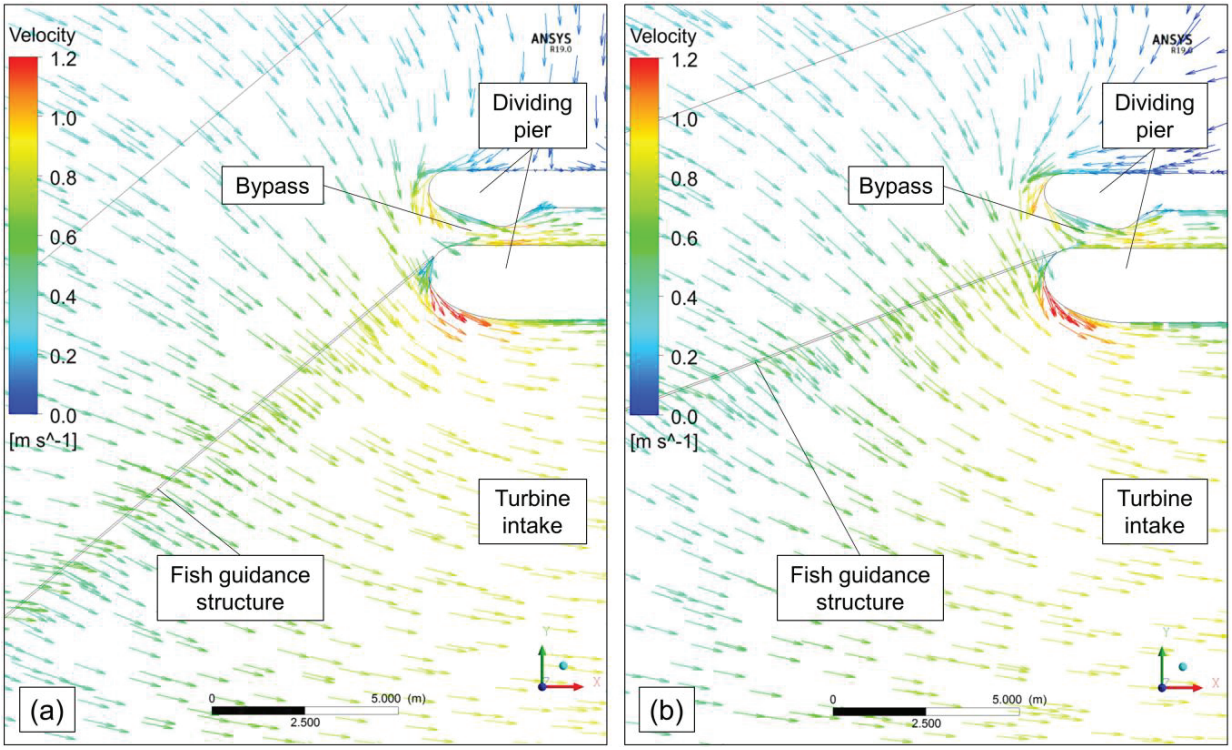

Figure 2. Velocity vectors (z = 2.0 m) at the lower end of the FGS with (a) α = 40° and (b) α = 20° to the unaffected flow direction at the block-type HPP on the pre-alpine river (HPP II) during normal operation in plan view

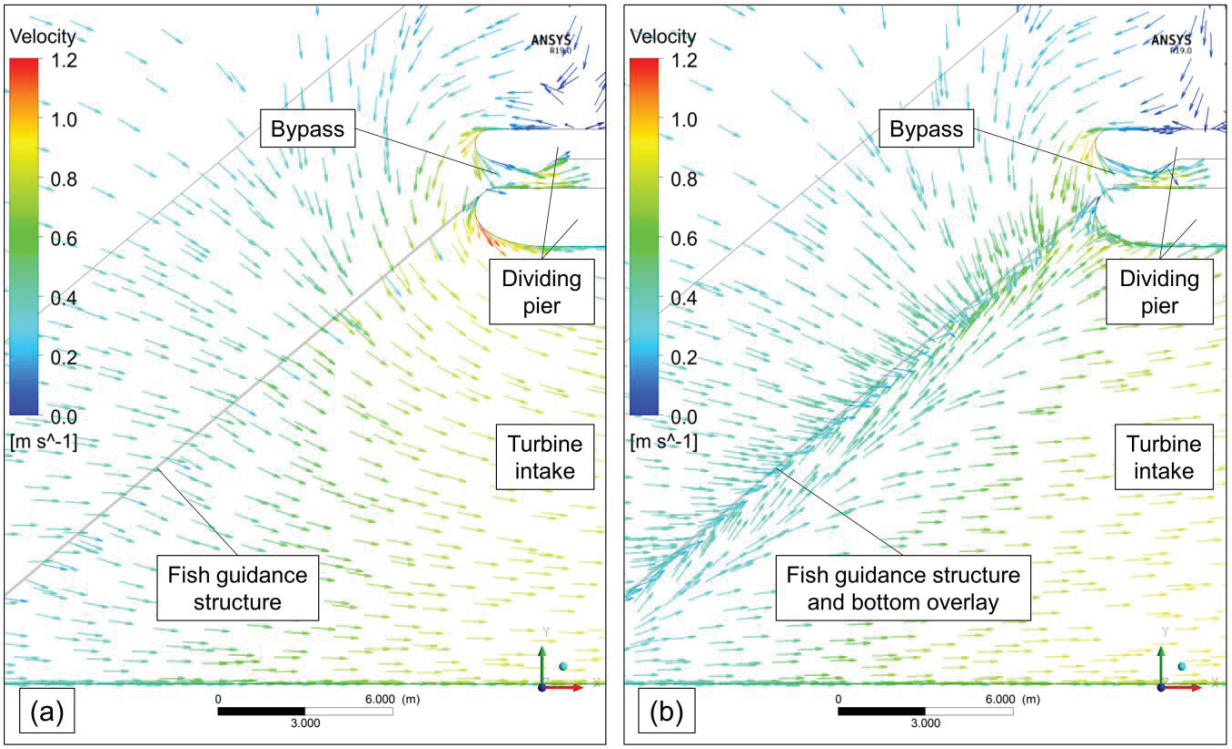

Figure 3. Velocity vectors (z = 0.1 m) in the vicinity of the FGS (a) without a bottom overlay and (b) with a bottom overlay at the block-type HPP on the pre-alpine river (HPP II) during normal operation in plan view

Bottom overlays have a fundamentally positive effect on FPE by increasing the barrier effect, especially for bottom-orientated fish. The FGE is also improved from an overall perspective, although the ability to find the bypass is worsened in Figure 3(b) by the additional slight deflection of the flow at the lower end of the FGS or the bottom overlay, respectively. However, it can be assumed that this deflection merely delays downstream migration of fish and does not result in any further negative effect on FGE. From a hydraulic point of view, the inclusion of a bottom overlay at a FGS can lead to further deflections of the turbine admission flow and increase the hydraulic losses associated with possible production losses in the operation of HPPs (Meister, 2020).

It should be noted that Figure 3(a) shows results from the same numerical simulation as Figure 2(a), but at different flow depths of observation. Significantly more favorable conditions regarding FGE occur at mid-depth (Figure 2a) than near the bottom (Figure 3a). In the presented variants, this effect can be explained by the bypass system used. In general, however, varying flow conditions at different flow depths can also occur, for example, depending on the type of turbines used. This results in different situations with respect to FGE and FPE for fish migrating downstream bottom-oriented or water surface-oriented.

3.4 Effect of The Position of The Dividing Pier

Figure 4 shows the velocity vectors at the lower end of the FGS with α = 40° to the unaffected flow direction at the bay-type HPP on the lowland river (HPP I) with different positioning of the dividing pier. Due to the angled bar rack bypass system designed by Ebel, Gluch & Kehl (2001) as described in Ebel (2018), the dividing pier is divided into a weir-side and a turbine-side part. In Figure 4(a), both parts are situated at the same level regarding the unaffected flow direction (*x*-direction). In Figure 4(b), the weir-side part of the dividing pier was moved 2 m upstream. The displacement leads to the velocity vectors in front of the bypass and at the lower end of the FGS pointing more in the direction of the bypass inlet. This results in more favorable conditions for FGE. However, the displacement increases the velocity around the weir-side part of the dividing pier and also at the lower end of the FGS. In addition, the bypass inlet becomes harder to find for fish in the area next to the weir. Based on these arguments, the displacement of the weir-side part shown in Figure 4(b) has a generally positive effect on the FGE, although this effect is significantly reduced by the increased flow velocities towards the FGS. Regarding the increased flow velocities, care must be taken not to exceed the critical limits depending on the key fish species to not adversely affect the FPE.

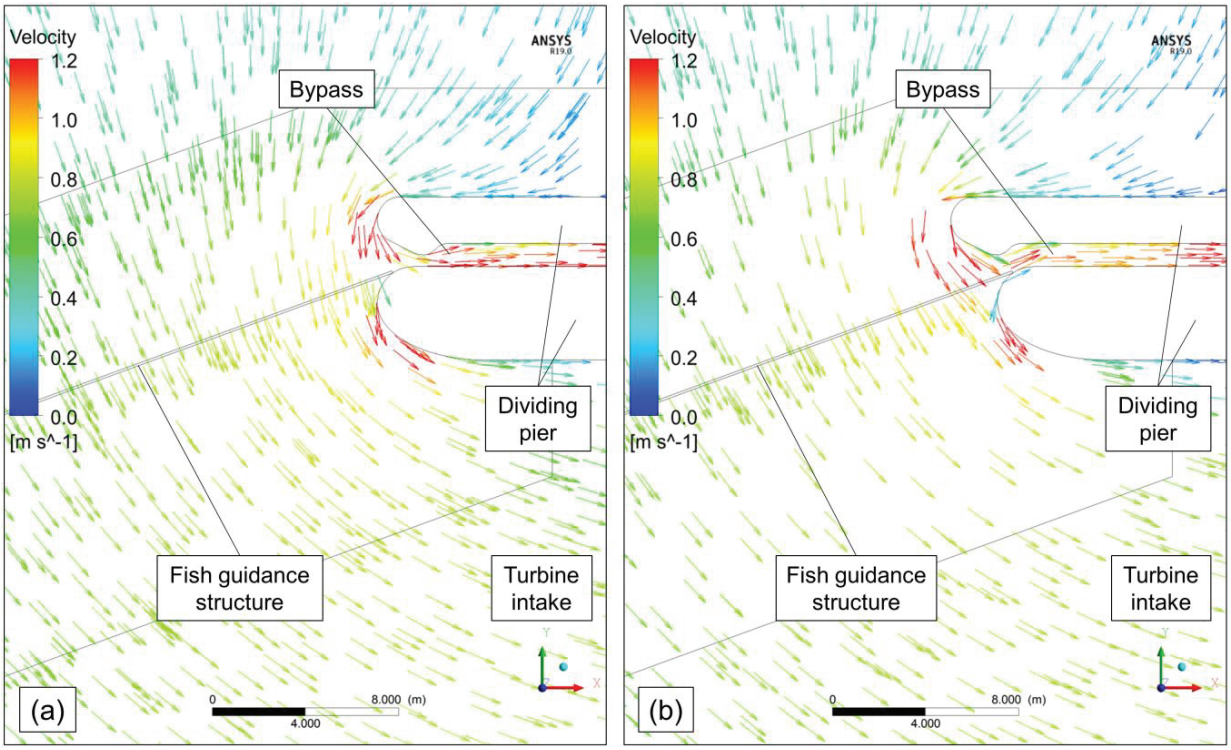

Figure 4. Velocity vectors (z = 2.5 m) at the lower end of the FGS (a) with both parts of the dividing pier at the same level in flow direction (*x*-direction) and (b) with the weir-side part moved 2 m upstream at the bay-type HPP on the lowland river (HPP I) during normal operation in plan view

In general, the dividing pier has a significant influence on the turbine admission flow at HPPs (Giesecke and Heimerl, 2014). Since the bypass is integrated in the dividing pier in the variants shown in Figure 4, the dividing pier also has a considerable influence on the downstream migration of fish. In this case, not only the position of the two parts is of importance, but also the shape of both parts. In Figure 4, the turbine-side part was designed for optimized flow in the direction of the turbines according to the design recommended by Häusler (1987) for the HPP Isarstufe Landau, Germany, while the weir-side part was simplified evenly rounded. Moreover, at the weir-side part, an integrated flap for controlling the discharge though the bypass was placed, which also significantly affects the flow conditions in the inlet area of the bypass. Within the research project, other variants with different positions and shapes of the dividing pier were investigated (Zöschg et al., 2021), which are not presented here.

3.5 Effect of Bypass Discharge

Figure 5 shows the velocity contours at the lower end of the FGS with α = 40° to the unaffected flow direction at the block-type HPP on the alpine river (HPP III) with the bypass discharges (a) Q_{by} = 0.5 m³/s and (b) Q_{by} = 1.0 m³/s. In Figure 5(a), the bypass flow discharge in relation to the total discharge was $Q_{by,rel}$ = 5%, in Figure 5(b) $Q_{by,rel}$ = 10%. Note that the bypass channel had a width of 1 m and was narrowed by half to 0.5 m at the level of the flap. From a hydraulic point of view, the variant with $Q_{by,rel}$ = 5% leads to unfavorable detachments in the vicinity of the flap before and after the constriction. In this area, the maximum flow velocities over the entire cross-section are also lower compared to those at the downstream end of the FGS. Thus, there is no increase in flow velocity from the FGS into the bypass, as recommended by Ebel (2018) for angled bar rack bypass systems. This has a negative influence on the FGE into the bypass. Increasing the bypass discharge rate to $Q_{by,rel}$ = 10% shown in Figure 5(b) leads to a slight increase in flow velocity into the bypass and to a slight reduction in flow velocities at the downstream end of the FGS. In terms of FGE and FPE, the variant with $Q_{by,rel}$ = 10% shows more favorable flow conditions.

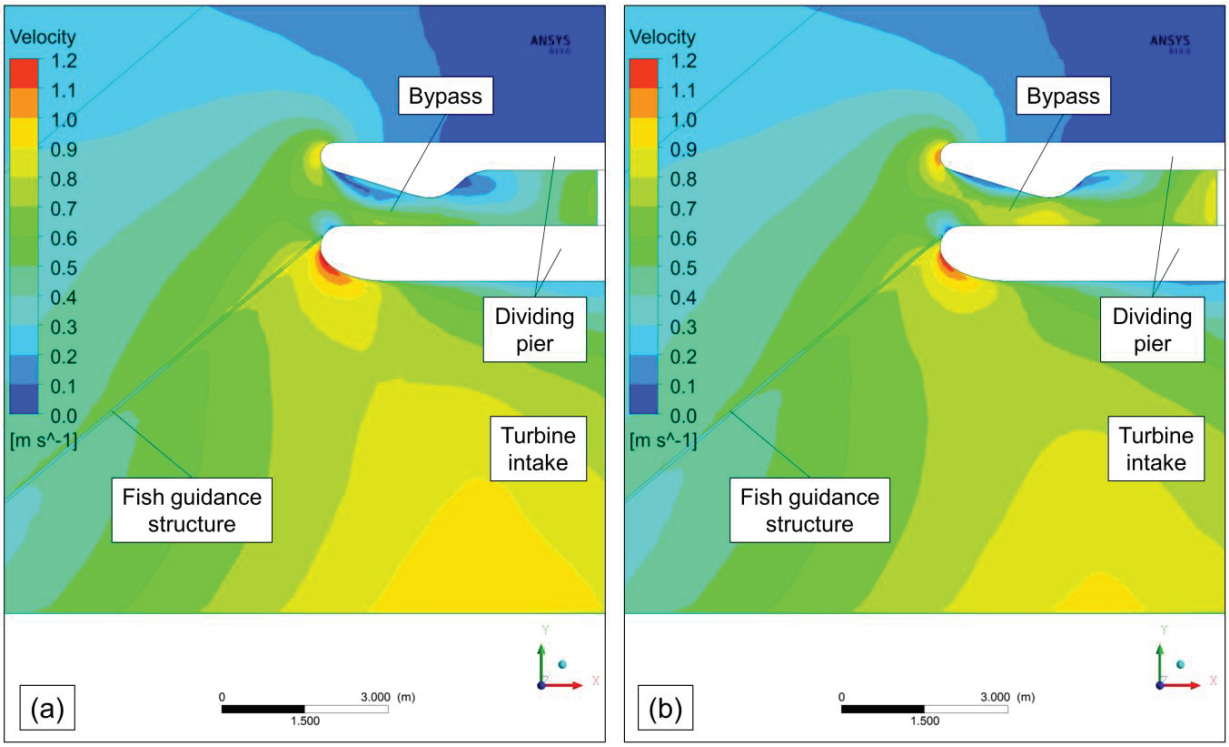

Figure 5. Velocity contours (z = 1.0 m) at the lower end of the FGS (a) with $Q_{by,rel}$ = 5% and (b) with $Q_{by,rel}$ = 10% at the block-type HPP on the alpine river (HPP III) during normal operation in plan view

As shown in Figure 5, the bypass discharge is essential to establish a good FGE along the FGS in direction of the bypass inlet. According to Ebel (2018), the discharge in the bypass should be at least $Q_{by,rel}$ = 2%. He recommended to define a suitable guiding flow in the direction of the bypass entrance as the decisive criterion. Therefore, especially for small HPPs like HPP III with a discharge of 10 m³/s, larger bypass discharges are needed to provide favorable flow conditions. Nevertheless, an increase in Q_{by} can lead to significant production losses. Further possibilities to optimize the flow conditions into the bypass are, for

example, changes to the geometry of the bypass, including an adjustment of the bypass width, considering the recommended values in the literature, or the geometry and position of the dividing pier (see 3.4).

3.6 Effect of The Type of Construction

Figure 6 shows the velocity vectors in the vicinity of the FGS with α = 20° to the unaffected flow direction (a) at the bay-type HPP on the lowland river (HPP I) and (b) at the block-type HPP on the pre-alpine river (HPP II). Note that Figure 6(a) presents the same data as Figure 4(a) and Figure 6(b) the same data as Figure 2(b) but in Figure 6 the velocity vectors near the entire FGS are presented. Further, the discharges of the two HPPs shown in Figure 6 are different as well as the height of the presented results. However, the similar flow velocities near the FGS allow a simplified general comparison. The block-type HPP (HPP II) has basically more favorable characteristics with respect to the FGE compared to the bay-type HPP (HPP I). The anthropogenically constructed bay results in increased flow angles to the FGS. Thus, despite the flat angled FGS, no tangential velocities can be detected at the lower end of the FGS at HPP I and no pronounced FGE in the direction of the bypass inlet is given. For this reason, it is necessary to reduce the flow velocities at the FGS to not adversely affect the FPE. In addition, the bay-type HPP (HPP I) is more likely to have deflected turbine admission flows due to the increased flow angles around the dividing pier, which can lead to production losses.

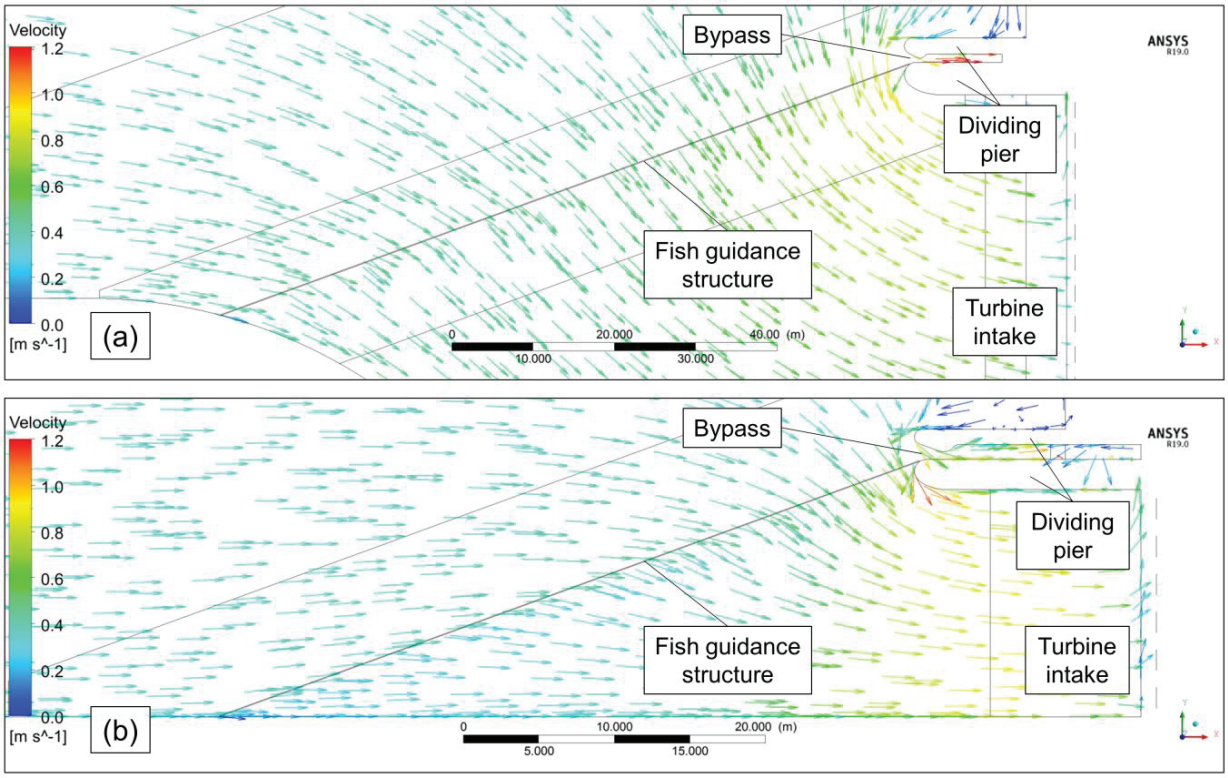

Figure 6. Velocity vectors in the vicinity of the FGS (a) at the bay-type HPP on the lowland river (HPP I; z = 2.5 m) and (b) at the block-type HPP on the pre-alpine river (HPP II; z = 2.0 m) during normal operation in plan view

From an economic point of view, the bay-type HPP has advantages over the block-type HPP due to the generally shorter length of the FGS with identical angle of the FGS. This also affects the construction and operation of the trash rack cleaning system. Moreover, from a general point of view, the bay-type HPP offers further advantages, for example, in rivers with high bedload transport or in case of flooding events (Giesecke and Heimerl, 2014).

4. CONCLUSIONS

In the planning of new run-of-river HPPs as well as in the ecological adaptation of existing ones, the protection of downstream migrating fish is of increasing importance. Suitable technical measures must be implemented to ensure that fish can safely migrate downstream. For example, an angled bar trash rack used as a fish guidance structure in combination with a bypass system. However, general solutions are still missing.

In order to provide general recommendations that go beyond the frequently applied “trial and error” approach (Katopodis and Williams, 2012), a numerical approach was used in the present study. Geometrical and hydraulic parameters at simplified low-head HPPs in the catchment area of the Austrian Danube river were varied, simulated numerically and subsequently evaluated regarding the fish guidance efficiency and the fish protection efficiency.

The results from the 3D numerical simulations show the effects of the presented geometric (i.e. rack angle, bottom overlay, position of the dividing pier and design type of HPP) and hydraulic (i.e. bypass-discharge) parameters on the flow conditions. For example, the block-type design generally causes less flow deflection compared to a bay-type design and therefore has conditions more favorable for fish guidance efficiency due to the lower approach flow angles to the fish guidance structures. In general, increased awareness is required at the lower end of the fish guidance structure and the bypass inlet. For all considered HPPs in normal operation in this study, the inflow to the fish guidance structures was almost perpendicular in that section, which negatively effects the fish guidance efficiency and the fish protection efficiency.

Flow conditions at run-of-river HPPs essentially depend on the species- and site-specific conditions. Therefore, an individual examination in the planning process is recommended. The 3D numerical approach presented in this study demonstrated the potential of numerical simulations in combination with fish biology data and behavioral correlations in the planning of measures for downstream migration of fish at run-of-river HPPs.

5. ACKNOWLEDGEMENTS

This study is part of the research project “Fish Protection and Inflow at Hydropower Plants with Low Head”, funded by the Austrian Research Promotion Agency (FFG) within the framework of the Energy Research Program (4. call). The computational results presented here have been achieved (in part) using the LEO HPC infrastructure of the University of Innsbruck.

6. REFERENCES

Aufleger, M., Brinkmeier, B., 2010. Das Konzept des Fließgewässerkraftwerkes. Österr Wasser- und Abfallw 62, 169–175 [in German]. https://doi.org/10.1007/s00506-010-0233-y.

BMK, 2020. Energie in Österreich 2020. Zahlen, Daten, Fakten. Bundesministerium für Klimaschutz, Umwelt, Energie, Mobilität, Innovation und Technologie, Wien [in German].

BMLFUW, 2017. Nationaler Gewässerbewirtschaftungsplan 2015. Bundesministerium für Land- und Forstwirtschaft, Umwelt und Wasserwirtschaft, Wien [in German].

BMLFUW, 2012. Leitfaden zum Bau von Fischaufstiegshilfen. Bundesministerium für Land- und Forstwirtschaft, Umwelt und Wasserwirtschaft, Wien [in German].

Böttcher, H., Gabl, R., Aufleger, M., 2019. Experimental Hydraulic Investigation of Angled Fish Protection Systems—Comparison of Circular Bars and Cables. Water 11, 1056. https://doi.org/10.3390/w11051056

Celik, I. B., Ghia, U., Roache, P. J., 2008. Procedure for Estimation and Reporting of Uncertainty Due to Discretization in CFD Applications. J. Fluids Eng. 130, 078001. https://doi.org/10.1115/1.2960953.

Ebel, G., 2020. Biologische Wirksamkeit von Leitrechen-Bypass-Systemen - Aktueller Kenntnisstand. Wasserwirtsch 110, 18–27 [in German]. https://doi.org/10.1007/s35147-020-0758-3.

Ebel, G., 2018. Fischschutz und Fischabstieg an Wasserkraftanlagen: Handbuch Rechen- und Bypasssysteme: ingenieurbiologische Grundlagen, Modellierung und Prognose, Bemessung und Gestaltung, 3. Auflage. ed, Mitteilungen aus dem Büro für Gewässerökologie und Fischereibiologie Dr. Ebel. Büro für Gewässerökologie und Fischereibiologie Dr. Ebel, Halle (Saale) [in German].

European Commission, 2000. Directive 2000/60/EC of the European Parliament and of the Council of 23 October 2000 establishing a framework for community action in the field of water policy. Official Journal of the European Communities, 22(12), 2000.

Feigenwinter, L., Vetsch, D., Kammerer, S., Kriewitz, C., Boes, R., 2019. Conceptual Approach for Positioning of Fish Guidance Structures Using CFD and Expert Knowledge. Sustainability 11, 1646. https://doi.org/10.3390/su11061646.

Giesecke, J., Heimerl, S., 2014. Wasserkraftanlagen: Planung, Bau und Betrieb, 6., aktualisierte u. erw. Aufl. ed, SpringerLink. Springer, Berlin, Heidelberg [in German].

Haug, J., 2018. Examination of the fish protection and guiding effect of the “electrified flexible fish fence” depending on the electrical field - comparison of the efficiency of the electrified flexible fish fence with 60 mm cable clearance and 20° angle of incidence according to ethohydraulic experiments in Lunz am See (Master’s Thesis). University of Innsbruck, Innsbruck.

Haunschmid, R., Wolfram, G., Spindler, T., Honsig-Erlenburg, W., Wimmer, R., Jagsch, A., Kainz, E., Hehenwarter, K., Wagner, B., Konecny, R., Riedmüller, R., Ibel, G., Sasano, B., Schotzko, N., 2006.

Erstellung einer fischbasierten Typologie österreichischer Fließgewässer sowie einer Bewertungsmethode des fischökologischen Zustandes gemäß EU-Wasserrahmenrichtlinie, Schriftenreihe des BAW, Band 23. Wien [in German].

Häusler, E., 1987. Wehre, in: Wasserbauten Aus Beton, Handbuch Für Beton-, Stahlbeton- Und Spannbetonbau. W. Ernst, Berlin [in German].

Katopodis, C., Williams, J.G., 2012. The development of fish passage research in a historical context. Ecological Engineering 48, 8–18. https://doi.org/10.1016/j.ecoleng.2011.07.004.

Meister, J., 2020. Fish protection and guidance at water intakes with horizontal bar rack bypass systems. ETH Zurich. https://doi.org/10.3929/ETHZ-B-000455545.

Szabo-Meszaros, M., Forseth, T., Baktoft, H., Fjeldstad, H., Silva, A.T., Gjelland, K.Ø., Økland, F., Uglem, I., Alfredsen, K., 2019. Modelling mitigation measures for smolt migration at dammed river sections. Ecohydrology 12. https://doi.org/10.1002/eco.2131.

Zöschg, H., Haug, J., Tutzer, R., Zeiringer, B., Unfer, G., Stoltz, U., Aufleger, M., 2021. Fischschutz und Anströmung an Wasserkraftanlagen mit niedrigen Fallhöhen. Wasserwirtsch 111, 36–42 [in German]. https://doi.org/10.1007/s35147-021-0891-7.

